Int. J. Nano Dimens., 7 (2): 150-159, Spring 2016

ORIGINAL RESEARCH PAPER

Synthesis of porous CdO sheet-like nanostructure based on soft template model and application in dye pollutants adsorption

Azadeh Tadjarodi *; *Mina Imani*

Research Laboratory of Inorganic Materials Synthesis, Department of Chemistry, Iran University of Science and Technology, 16846-13114, Tehran, Iran

Received 19 October 2015; revised 13 January 2016; accepted 26 January 2016; available online 06 May 2016

ABSTRACT: In this work, the synthesis of porous structure of cadmium oxide with multilayered sheet-like morphology in nano-meter size using adipic acid as soft template by solvothermal/thermal decomposition process is reported. Chemical analyses exhibited that the formation of porous sheet-like structure is originated from bidentate coordination mode of adipate units to Cd-center. It was found that the change of reaction conditions can vary final morphology of product due to the different coordination modes of adipate units. The structural and morphological characterizations of product were discussed in detail. Brunauer-Emmett-Teller (BET) analysis indicated a specific surface area of 52.08 m^2g^{-1} with pore size distribution centered at 11.7 nm for prepared CdO sheet-like nanostructure. The capability of the as prepared product for adsorption of dye pollutants from aqueous solution was also studied. The results showed a maximum adsorption capacity (q_{max}) of 500 mg g^{-1} for adsorption of Congo Red (CR) dye in water revealing a superior ability of this product for adsorption of dye pollutants.

Keywords: *Adsorption ; CdO; Nanostructure; Soft template; Solvothermal process*

How to cite this article
Tadjarodi A, Imani M. Synthesis of porous CdO sheet-like nanostructure based on soft template model and application in dye pollutants adsorption. 2016; 7(2): 150-159. DOI: 10.7508/ijnd.2016.02.007

INTRODUCTION

On the other hand, the use of soft chelating templates under solvothermal/hyndrothermal reactions simplicity can direct the synthesis pathway towards design and engineering of metal oxide architectures with special morphologies. Poly carboxylic acids such as trimesic, isophetalic, pyromellitic, succinic and adipic acids are a known class of chelating polycarboxylate agents with efficient ability of different coordination modes so that can be selected to produce precursors for various nanostructured metal oxides [11-13]. Such precursors can easily transform to oxide form by a simple thermal decomposition using rather low energy. As a matter of fact, the synthesis of porous CdO sheet-like nanostructure using adipate template model has not yet been reported. One of the important applications of metal oxides is in decolorization of organic dye pollutants from water [14-16]. Organic dyes are a common class of harmful pollutants resulting from different industries, which should be refined and removed before their discharge to the environment. Adsorption process is an effective, simple and economical route for decolorizing wastewaters from aqueous solutions. Although the adsorption process of colored pollutants using metal oxides is not a new study, this operation is still interesting for researchers to mature it. The use of CdO nanostructure for this operation shows to be possible with positive results. We used the prepared porous CdO sheet-like nanostructure for adsorption of Congo red (CR) as a model contamination in water. Molecular structure of the mentioned dye has been illustrated in Fig. 1.

*Corresponding Author: *Azadeh Tadjarodi*
Email: *i_shoaie@yahoo.com*
Tel.: (+98) 21 77240359; Fax: (+98) 21 77491204

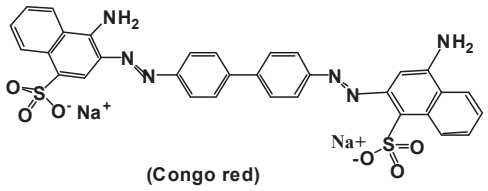

Fig. 1: Molecular structure of Congo red (CR) dye.

EXPERIMENTAL

Materials of synthesis

Cadmium nitrate tetrahydrate ($Cd(NO_3)_2.\ 4H_2O$, Merck, pure), and adipic acid (Hexanedioic acid, $C_6H_{10}O_4$, Merck, pure) were supplied as initial reagents to synthesize Cd-precursor and CdO nanostructure. Methanol (Merck, 98% purity) and N,N-Dimethyl formamide, DMF, (C_3H_7NO , Merck, pure) were used as solvent. Congo Red (disodium 4-Amino-3-[4-[4-(1-amino-4-sulfonato-naphthalen-2-yl)diazenylphenyl]phenyl]diazenyl-naphthalene-1-sulfonate) was utilized as model dye for study of adsorption capability of product.

Characterizations

The powder X-ray diffraction (XRD) measurements were carried out by a JEOL diffractometer with monochromatized Cu Kα radiation (λ=1.5418 Å). Fourier transform infrared (FT-IR) spectra were recorded on a Shimadzu-8400S spectrometer in the range of 400-4000 cm^{-1} using KBr pellets. Scanning electron microscopy (SEM) and energy dispersive X-ray (EDX) images were obtained on a Philips (XL-30) with gold coating. Thermogravimetric analysis (TGA) measurement was carried out on a TGA-Perkin Elmer Pyris-U.S apparatus with a heating rate of 10 ˚C min^{-1} under nitrogen atmosphere. Elemental analysis was performed by utilizing a FOSS Heraeus CHN microanalyser. Brunauer-Emmett-Teller (BET) surface area was performed by Micromeritics (Gemini) using nitrogen as the adsorbing gas. A double-beam UV spectrophotometer (Shimadzu UV-1700) was used for determination of CR concentration in the supernatant solutions before and after adsorption.

Synthesis methods

To prepare CdO sheet-like structure, the synthesis of Cd-precursor compound was designed using adipic acid as the chelating agent. At first, the amounts of adipic acid and $Cd(NO_3)_2.\ 4H_2O$ (with a molar ratio of 1:1) were mixed and dissolved in 20 mL of solvent. This solution was sealed in Teflon-lined stainless steel vessels (80 mL) and treated at 140 ˚C for 5 days. The resulting precursor was filtered, washed, dried and characterized. The obtained precursors were calcined at 400 ˚C for 2 h to obtain porous CdO sheet-like nanostructure. The change of reaction conditions on the produced structure was studied in different temperature-time programs (shown in Table 1). The prepared products were characterized by FT-IR, XRD and SEM analyses.

Adsorption test

Adsorption process was performed under following conditions: 0.01 g of the prepared nanoporous CdO structure was added to 25 mL of CR dye aqueous solution (with the initial concentration of 10 mg L^{-1} to 500 mg L^{-1}, neutral pH) and stirred for 2 h in dark. Then, in the specified interval, the portions of supernatant were taken away from adsorbent and the concentration of the residual dye was measured by UV-Vis spectrophotometer at an appropriate wavelength corresponding to the maximum absorption of CR (498 nm).

RESULTS AND DISCUSSION

Structural Description of samples

Fig. 2 exhibits FT-IR spectra of the resulting CdO nanostructures after thermal decomposition of the prepared Cd-precursors at 400 ˚C for 2. According to this analysis, the all of organic functional groups were disappeared due to heat treatment and no typical absorption band is observed. It reveals the presence of only CdO phase [8, 14]. To obtain the suitable decomposition temperature to reach metal oxide phase, we performed TGA analysis from precursor (A) as a typical sample (Fig. 3).

According to this curve, Cd-precursor is decayed in a two-step pattern of weight loss. The first partial weight loss of 3 % is observed in the range of 150-300 ˚C, which can be related to the decomposition of the adsorbed water molecules. The second major weight loss of 35% appeared in the range of 300-400 ˚C can be attributed to the decomposition of the organic sections in the precursor structure. Since the weight loss process terminates at 400 ˚C, this temperature was determined as heat treatment temperature of the intermediate molecules to obtain CdO phase. In addition, DTA spectrum corresponding to TGA curve (Fig. 3) reveals a sharp exothermic peak

at 380 ˚C. It demonstrates the loss of heat in this temperature according to the second step of weight loss in the TGA curve revealing the presence of only one phase transition from intermediate to CdO phase.

The prepared Cd-precursors were characterized by FT-IR spectra and CHN elemental analysis. Fig. 4 depicts FT-IR spectra of the resulting precursors from three reaction conditions according to Table 1. These spectra indicated the successful coordination of adipate units to Cd (II) cation and the formation of the desired precursors. The appeared peaks are related to the presence of theorganic functional

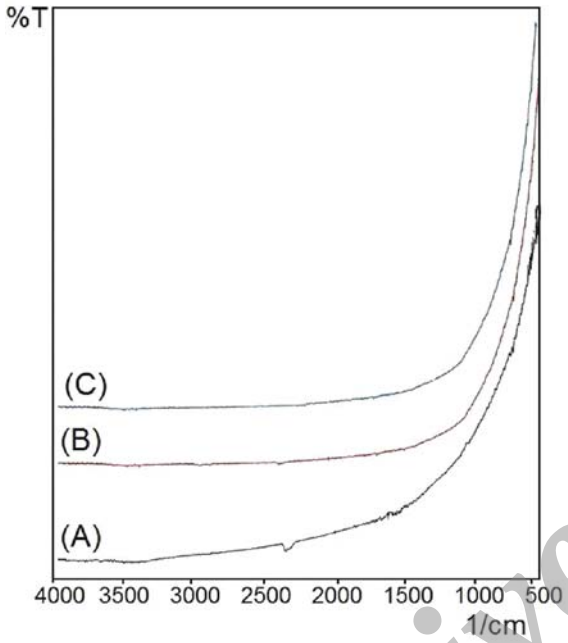

Fig. 2: FT-IR spectra of the obtained CdO nanostructures after calcination at 400˚C for 2 h.

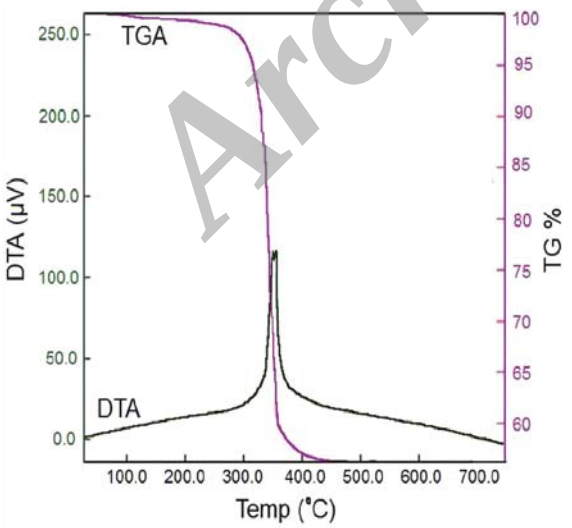

Fig. 3: TGA curve and DTA from the sample (A).

Table 1: Programmed temperature-time terms to prepare precursors and related CdO structures

Course	Temperature (℃)	Time (days)	CdO structure After calcination
(A)	160	2	Block-like microstructure
(B)	160	5	Nanoparticles
(C)	140	5	Porous nanosheets

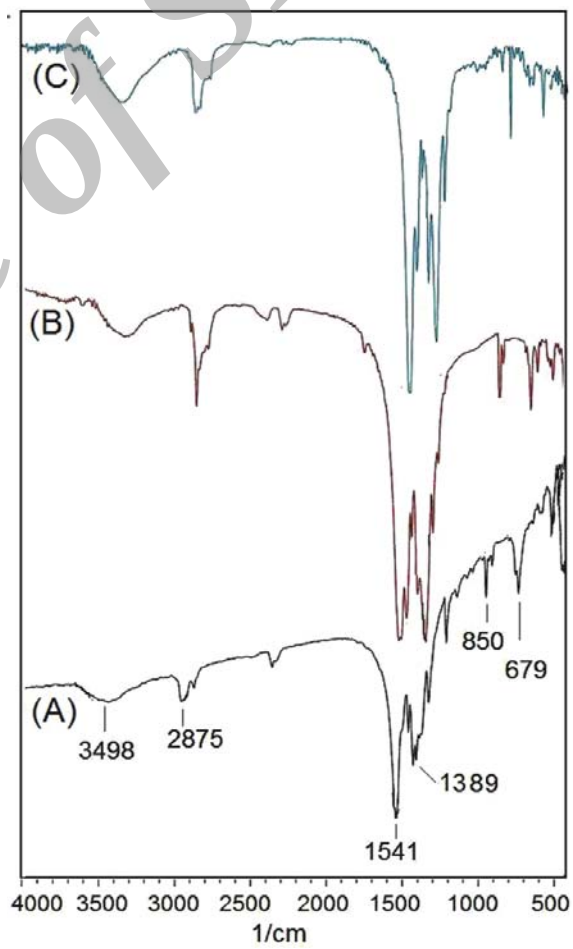

Fig. 4: FT-IR spectra of the prepared Cd-precursors of (A), (B) and (C).

groups in precursor structures. peak at 850 cm^{-1} is related to C-O bending vibration. Based on literature the difference value of ν_a (COO^-) and ν_s (COO^-) in unidentate coordinated compouns is greater than ionic compound and bidentate one shows the less difference value [17].

Table 2 indicates the related frequencies to these parameters and probable coordination modes of adipate unit to Cd-center. Based on these results, samples (A) and (C) represent the bidentate modes of coordination and sample (B) indicates unidentate coordination mode. In addition, vibration frequency peaks of coordinated nitrate unit are observed at 1000 to 1476 cm^{-1}.

Elemental analysis was used to determine molecular formula of the synthesized precursors. These data are summarized as follow:

Anal. Calcd. for sample (A):

$[Cd_2(C_6H_8O_4)](NO_3)_2(CH_3OH)$: C, 15.41: H, 2.20: N, 5.13 (%). Found: C, 15.87: H, 2.24: N, 6.17 (%).

Anal. Calcd. for sample (B):

$[Cd_{72}(C_6H_8O_4)_{36}](NO_3)_2$: C, 19.30: H, 2.08: N, 0.20 (%). Found: C, 18.77: H, 1.56: N, 0.17 (%).

Anal. Calcd. for sample (C):

$[Cd_{57}(C_6H_8O_4)_{56}.(C_6H_9O_4)_2]$: C, 27.17: H, 3.05: N, 0.00 (%). Found: C, 26.98: H, 2.68: N, 0.00 (%).

According to the aforementioned data, the formula of the prepared intermediate molecules for samples (A), (B) and (C) are $[Cd_2(C_6H_8O_4)](NO_3)_2(CH_3OH)$, $[Cd_{72}(C_6H_8O_4)_{36}](NO_3)_2$ and $[Cd_{57}(C_6H_8O_4)_{56}.(C_6H_9O_4)_2].(H_2O)_2$, respectively. The probable structures of these compounds were illustrated in Fig. 5. The carboxylate functional groups are engaged as a bidantate fashion in samples (A) and (C) and unidentate mode in sample of (B). The recorded XRD patterns for all prepared products after calcination shown in Fig. 6 clarify the solid state transformation and confirm the formation of CdO phase. These patterns display the formation of CdO phase with a lattice parameter a=4.695 Å (JCPDS card no. 05-0640). The diffraction peaks at 2θ values of 33.01°, 38.20°, 55.20°, 65.80° and 69.20° are in a close agreement with the 111, 200, 220, 311 and 222 planes of cubic cadmium oxide phase. No other peaks related to the impurities are detected.

Fig. 7a and b represent SEM images of resulting CdO nanostructure from sample (A). These images revealed block-like microstructure consisting of nanoparticles. The change of the precursor synthesis conditions led to the change of the resulting morphologies from block-like microstructure to the arranged nanoparticle and porous sheet-like microstructure (Fig. 7 c-f). The sheets indicate a porous morphology with the length of several micrometers and width of 200 nm composed from particles with an average size of 28 nm (Fig. 7e and f). The average size particle size was determined using a Microstructure Measurement program. As a result, the use of linear aliphatic chelating agent (adipic acid) causes to produce the chain-like structure of the precursor and form CdO sheet-like structure. In fact, the change of reaction conditions such as temperature and time under autogenous pressure supplies a suitable media to engage the poly dentate ligand to Cd-center and forms the unique structures.

Fig. 8 indicates the nitrogen adsorption and desorption experiments performed for the resulting porous sheet-like nanostructure to evaluate the surface area of this product. We recorded a distinct hysteresis loop at the range of $0<P/P_0<1$, which indicates the category of type V.

The Brunauer-Emmett-Teller (BET) surface area was calculated about 52.08 m^2g^{-1} for this product. The Barrett-Joyner-Halenda (BJH) model was used by using desorption branch of the nitrogen isotherm to evaluate the pore size distribution of sheet-like nanostructure (sample (C)). BJH plot inserted in the inset of Fig. 8 reveals that the pore size distribution for this nanostructure is centered at 11.7 nm. These results reveal a mesoporous structure. Therefore, this product can be nominated as a good adsorbent to

Table 2: Stretching vibration frequencies and probable coordination modes in precursors

Compound	ν_a (COO^-) (cm^{-1})	ν_s (COO^-) (cm^{-1})	$\Delta = [\nu_a (COO^-) - \nu_s (COO^-)]$ (cm^{-1})	Structure
CH_3COO^-	1578	1414	164	Ionic
Sample (A)	1541	1389	152	Bidentate
Sample (B)	1554	1371	183	Bidentate
Sample (C)	1542	1393	161	Unidentate

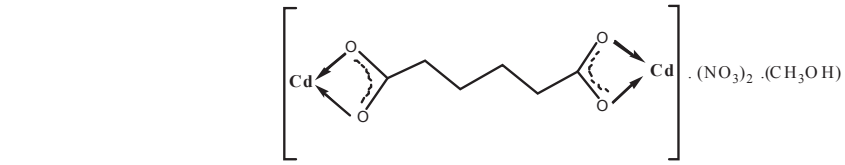

Sample (A)

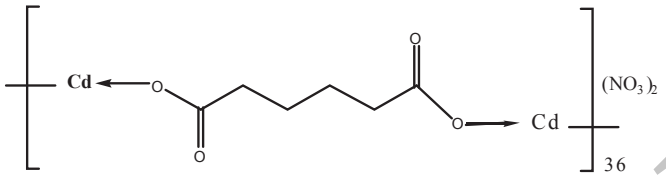

Sample (B)

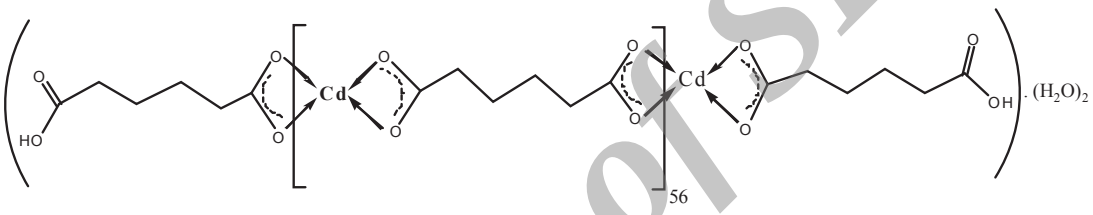

Sample (C)

Fig. 5: The probable structural fashions of the adipate ligand to Cd center in sample (A), (B) and (C).

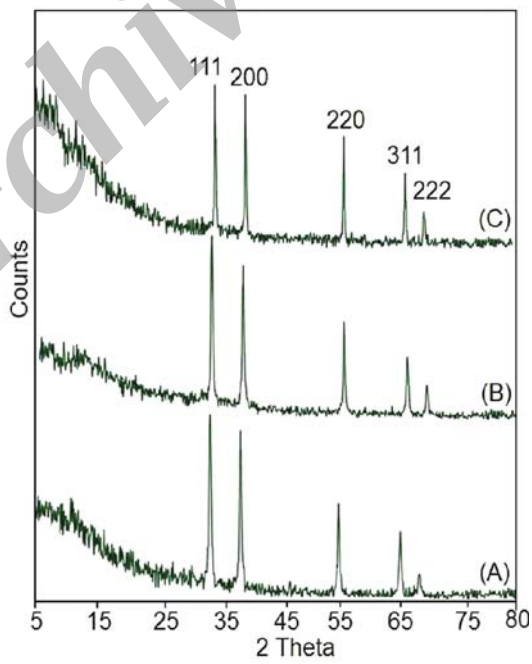

Fig. 6: XRD patterns of the prepared samples (A), (B) and (C) after heating treatment.

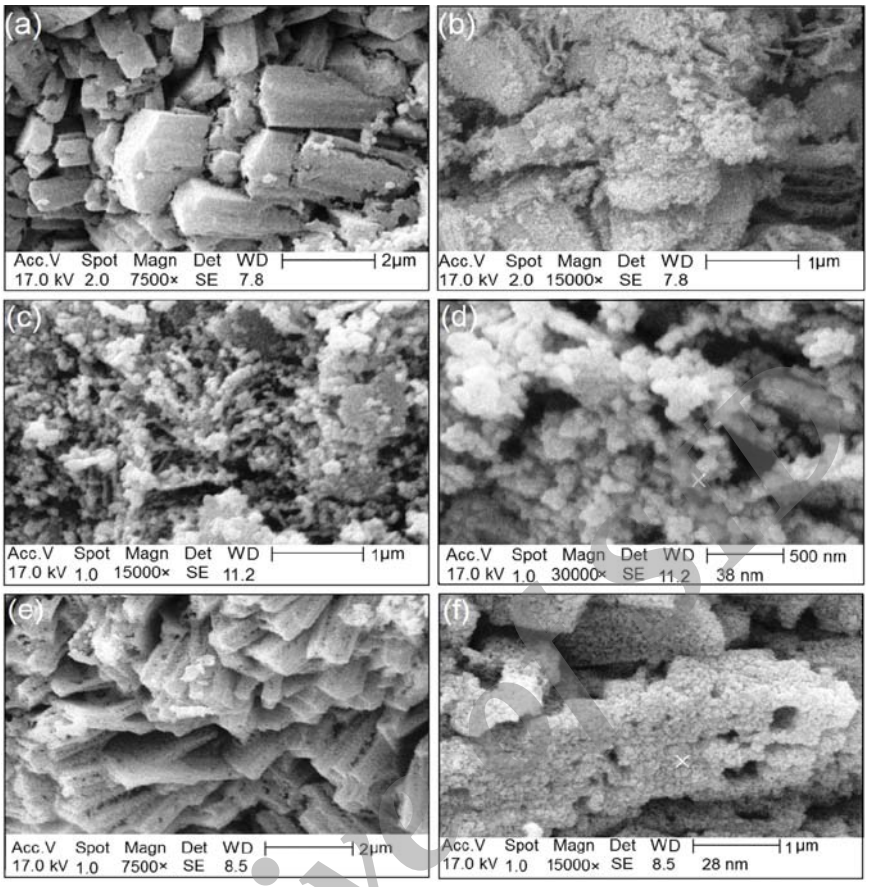

Fig. 7: SEM images of the obtained CdO nanostructures from sample (A) shown in a and b, sample (B) presented in c and d and sample (C) shown in e and f.

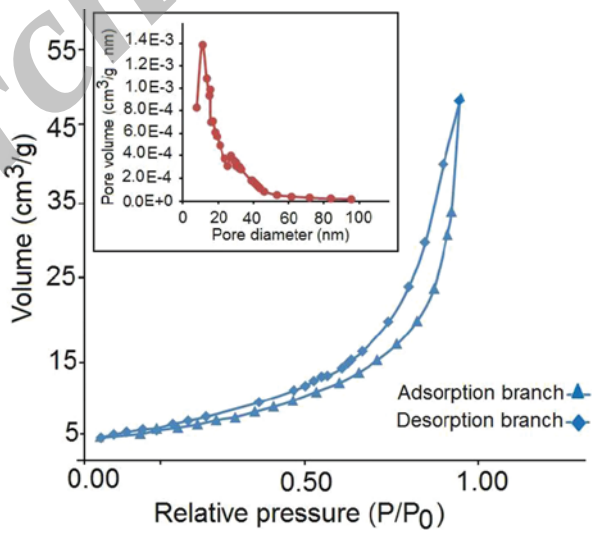

Fig. 8: Nitrogen adsorption (▲) and desorption (◆) isotherms for CdO porous nanosheet architecture. The inset shows BJH plot of this product.

remove the organic dye pollutants from aqueous solutions by adsorption mechanism.

Adsorption study

With reference to the obtained structure in experimental section, sample C was picked out for adsorption studies. It is expected that the mentioned structure shows a suitable adsorption capability due to rather high surface area and numerous available active sites.

The decolorizing percentage of dye pollutant from water is calculated by the following equation [16]:

$$\%\ \text{Decolorizi ng efficiency} = \frac{C_0 - C_t}{C_0} \times 100 \quad (1)$$

Where, C_0 is the initial concentration of dye and C_t is the concentration of dye after treatment at the different time, t.

The contact time effect of the adsorbent in CR solution (50 mgL^{-1} concentration) in the range of 0.5-2h was investigated to determine the optimum time for removing the colored particles at neutral pH. A certain amount of the prepared CdO nanostructure was added into a 25 mL of CR solution. Adsorption of CR molecules on the adsorbent sites led to a decrease in the concentration of CR with time (Fig. 9).

According to this diagram, the maximum removal efficiency of CR dye (nearly 100%) occurs about 2h for sample C. Therefore, this agitation time was selected for further studies. The effect of the adsorbent amount required for the maximum recovery of CR dye is shown in Fig. 10. Various quantities of the CdO nanostructure (sample C) were investigated in the range of 0.005 to 0.02 g at optimum time of 2h. Maximum recovery percentage was specified when 0.01 g of CdO nanoporous sheets was used in 25 mL solution of CR dye with 50 mgL^{-1} concentration at neutral pH. Therefore, further studies were conducted on CR dye at the optimum amount of the mentioned adsorbent.

Although pH is a significant controlling parameter that intensely influences the adsorption efficiency, this type of adsorbent represents excellent adsorption behaviour at neutral pH.

Fig. 11 describes the situation of removal efficiency under diverse pHs. According to this diagram, the prepared adsorbent has a same performance due to increase or decrease of pH in solution.

Adsorption capacity of the as prepared CdO nanostructure for CR solution is exhibited in Fig. 12. The initial and final concentrations of CR solution were studied after 2 h agitation in the dark. It was found that the adsorption of CR molecules increases with an enhancement in dye concentration and reach the saturation point at the high concentrations of 300, 400 and 500 mg L^{-1}. Langmuir and Freundlich equations, the famous adsorption isotherm models, were used to examine the relationship between the amount of CR adsorbed onto CdO sites and its equilibrium concentration in solution. In fact, these adsorption isotherms were employed to interpret the interactions between CR molecules and adsorbent.

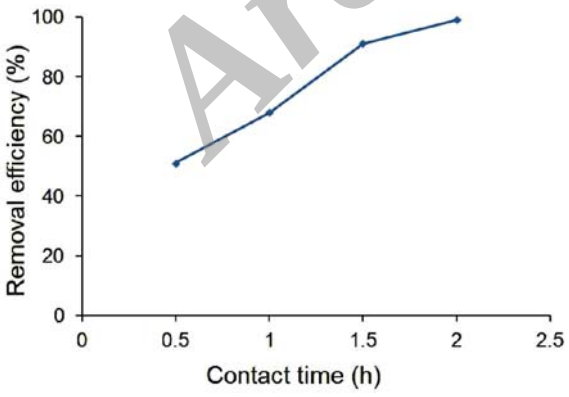

Fig. 9: Removal of CR dye in various times (0.5-2h). Conditions: 0.01 g CdO nanosheet structure, 25 mL of 50 mg L^{-1} CR solution and neutral pH.

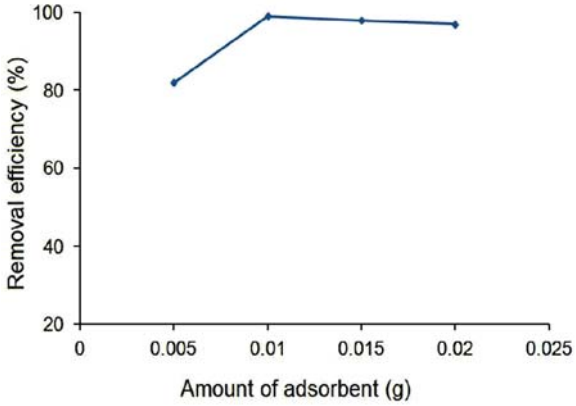

Fig. 10: The Effect of amount of adsorbent on the adsorption of CR.

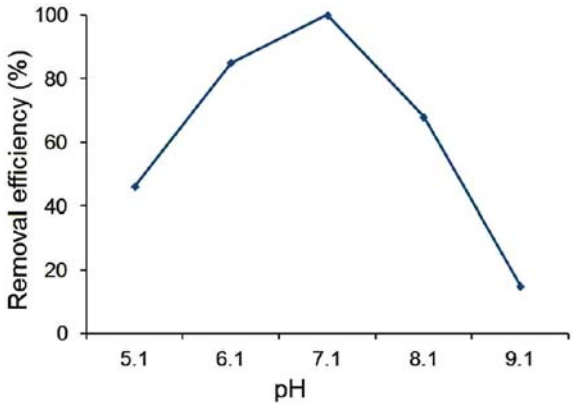

Fig. 11: The adsorption amount of CR in various pHs. Conditions: 0.01 g CdO nanostructure,25 mL of 50 mg L^{-1} CR.

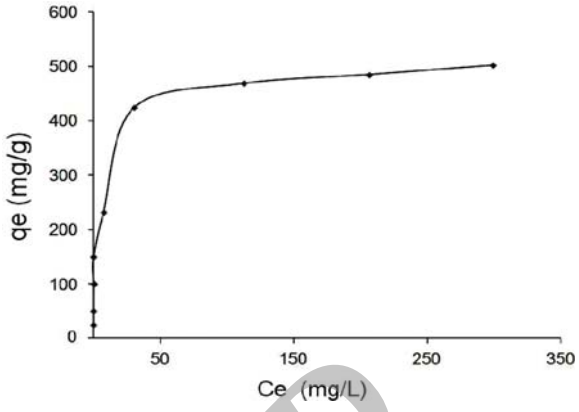

Fig. 12: The adsorption isotherm for Congo red (CR) on the prepared CdO porous nanosheets.

The linear forms of Langmuir (Eq. (2)) and Freundlich (Eq. (3)) isotherm models are as follow [16]:

$$\frac{C_e}{q_e} = C_e(\frac{a_L}{K_L}) + (\frac{1}{K_L}) \quad (2)$$

$$Log\ q_e = Log\ K_F + \frac{1}{n}\ Log\ C_e \quad (3)$$

The parameters of these two isotherm models were calculated and given in Table 3, where, a_L (Lmg^{-1}) and K_L (Lg^{-1}) are the Langmuir constants. These constants were calculated from the slope and intercept of the plot of C_e/q_e vs. C_e shown in Fig. 13a. Freundlich adsorption isotherm constants (K_F ($mg^{1-1/n}L^{1/n}g^{-1}$) and n) were obtained from the slope and intercept of linear plot of Log q_e vs. Log C_e (Fig. 13b). In these equations, C_e is the equilibrium concentration of the CR in the solution (mg L^{-1}). Meanwhile, q_e, the amount of CR adsorbed (mg g^{-1}) per unit of adsorbent at equilibrium (mg g^{-1}), is calculated by the following equation (4):

$$q_e = \frac{V(C_i - C_f)}{m} \quad (4)$$

Where, C_i and C_f are the initial and final concentrations of CR in mg L^{-1}, respectively; V is the volume of experimental solution in L, and m is the weight of CdO nanostructure in g.

The results indicated that this adsorption process dose not follow the Freundlich isotherm model, but it is in a good agreement with Langmuir model with reference to the obtained value of regression coefficients (R=0.9989). Although Langmuir's model does not consider the variation in adsorption energy, it obviously describes the adsorption method. It is based on the physical theory and monolayer adsorption of CR molecules on used adsorbent [14, 16].

Maximum adsorption capacity (mg g^{-1s}), q_{max}, is indicated by [$q_m = K_L/a_L$]. There is a relationship between q_{max} and the adsorbent structure so that the structures with more available sites can make more qualified adsorption. q_{max} for adsorption of CR onto porous CdO nanostructure was found to be 500 mg g^{-1}. This value is high acceptable value compared with the some reported adsorbents (Table 4).

To explain the essential characteristics of the presented Langmuir isotherm, a dimensionless constant separation factor (R_L) was used (Eq. (5)) [15]:

$$R_L = \frac{1}{(1 + K_L C_0)} \quad (5)$$

Generally, the nature of adsorption process can be described by several terms of R_L value; unfavourable ($R_L > 1$), linear ($R_L = 1$), favourable ($0 < R_L < 1$) and irreversible ($R_L = 0$). The obtained R_L value of 0.034 revealed that the adsorption performance of CR on the CdO nanosheets is a favourable process.

Adsorption kinetics

Fig. 14 represents two kinetic models of pseudo-first-order (Fig. 14a) and pseudo-second-order (Fig. 14b)

Table 3: Parameters of Langmuir and Freundlich isotherm equations, correlation coefficients (r) for adsorption of CR on CdO nanoporous sheets at 25 °C and neutral pH.

Langmuir model				Freundlich model		
a_L(L mg^{-1})	K_L(L g^{-1})	q_{max}(mg g^{-1})	R^2	K_F (mg$^{1-1/n}$ L$^{1/n}$ g^{-1})	n	R^2
0.286	142.857	500	0.998	166.265	4.817	0.903

Table 4: Summary of reported CR adsorption capacities of various adsorbents.

Type of adsorbent	q_{max}(mg.g^{-1})	Reference
CTAB-Kaolin	24.46	[18]
Jute Stick Powder	134.4 mg/g	[19]
Maghemite nanoparticles	208.33	[16]
α-FeOOH hollow spheres	275	[20]
CdO Nanoporous sheets	500	Present work

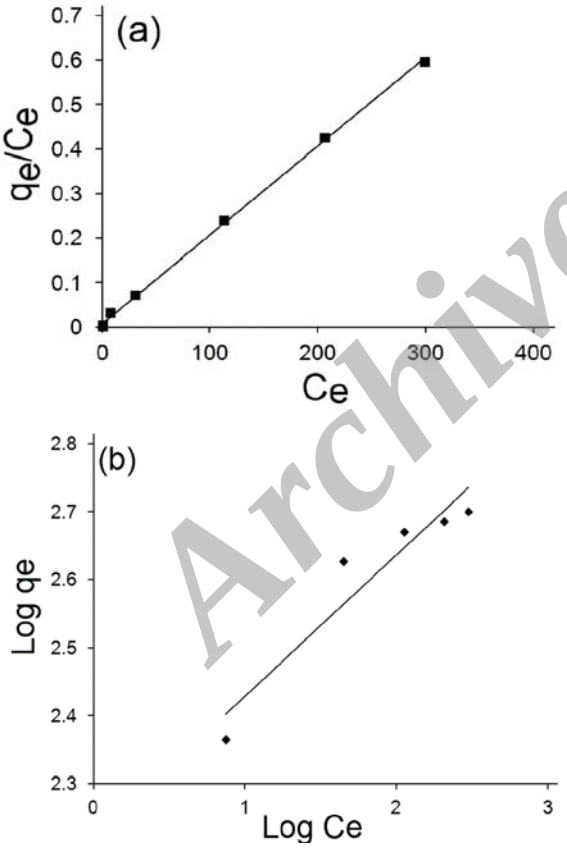

Fig. 13: The Langmuir (a) and freundlich (b) adsorption isotherms for the adsorption of CR, conditions: ambient temperature, neutral pH, 25 mL of CR dye with known initial concentrations (in the range of 50 mg L^{-1} to 500 mg L^{-1}) and 0.01 g of adsorbent.

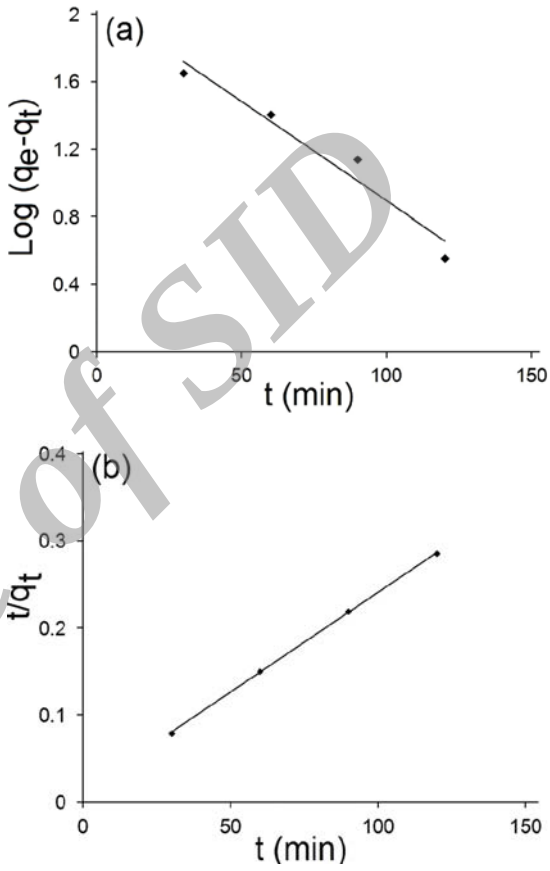

Fig. 14: The kinetic models for the adsorption of CR on the CdO porous nanosheets; (a) Pseudo-first-order and (b) Pseudo-second-order (conditions: ambient temperature, neutral pH, the initial CR dye concentration of 200 mg L^{-1} and 0.01 g of adsorbent).

rate equations of adsorption process from CR dye on the prepared adsorbent as follow [14, 16]:

$$\text{Log}\ (q_e - q_t) = \text{Log}\ q_e - \frac{k_1 t}{2.303} \quad (6)$$

$$\frac{t}{q_t} = \frac{1}{k_2 q_e^2} + \frac{t}{q_e} \quad (7)$$

Where, q_e and q_t are the amount of dye adsorbed (mg g^{-1}) at equilibrium and time, t (min), respectively. The parameters of k_1 and k_2 are the rate constants of pseudo-first-order (min^{-1}) and pseudo-second-order (g mg $^{-1}$ min^{-1}) equations, which were calculated from the linear plots of $log(q_e - q_t)$ vs. t and (t/q_t) vs. t, respectively. Table 5 shows the calculated kinetic parameters of both rate models. The comparison of the correlation coefficients (R^2) of the mentioned models revealed that the pseudo-second-order rate model is a better fit than the pseudo-first-order. This good agreement to the pseudo-second-order kinetic model can present the dependence of adsorption mechanism on the adsorbent structure. Although it is reported that the cadmium containing compounds are toxic to environment, we observed no realise of cadmium ion in system after separation of adsorbent from.

CONCLUSION

In a summary, we designed the synthesis of special nanostructure of CdO using soft template model. The synthesis of coordinated compounds using adipic acid as a chelating agent was exactly centered to this aim. The results showed that the coordination mode of chelating agent in precursor molecules can direct the synthesis pathway towards special morphologies of product. It can be attended in large amount production of special structures of metal oxides in nano meter size to use in various applications. As a typical study, we indicated high adsorption capacity of the as prepared CdO nanostructure in removal of CR dye pollutant from water.

ACKNOWLEDGEMENTS

The financial support of this study, by Iran University of Science and Technology and Iranian Nanotechnology Initiative, is gratefully acknowledged.

REFERENCES

1. Wei L., Peng X., HuaCong Z., LiangRong Y., Zhou L. H., (2012), Advanced functional nanomaterials with microemulsion phase. *Sci. China Tech. Sci.* 55: 387-416.
2. Haouemi K., Touati F., Gharbi N., (2011), Characterization of a New TiO2 Nanoflower Prepared by the Sol–Gel Process in a Reverse Microemulsion. *J. Inorg. and Organometal. Polym.* 21: 929-936.
3. Yakuphanoglu F., (2010), Nanocluster n-CdO thin film by sol-gel for solar cell applications. *Appl. Surf. Sci.* 257: 1413-1420.
4. Yakuphanoglu F., Caglar M., Caglar Y., Ilican S., (2010), Electrical characterization of nanocluster n-CdO/p-Si heterojunction diode. *J. Alloys Comp.* 506: 188-193.
5. Usharani K., Balu A. R., Suganya M., Nagarethinam V. S., (2015), Cadmium Oxide thin films deposited by a simplified spray pyrolysis technique for optoelectronic applications. *J. Appl. Chem. Res.* 9: 47-63.
6. Tadjarodi A., Salehi M., Imani M., (2015), Innovative one pot synthesis method of the magnetic zinc ferrite nanoparticles with a superior adsorption performance. *Mat. Lett.* 152: 57-59.
7. He Y., Wu Y., (2010), Evolution of MoTeOx/SiO2 and MoBiTeOx/SiO2 catalysts in the partial oxidation of propane to acrolein. *Appl. Surf. Sci.* 256: 4317–4321.
8. Tadjarodi A., Imani M., Kerdari H., (2013), Experimental design to optimize the synthesis of CdO cauliflower-like nanostructure and high performance in photodegradation of toxic azo dyes. *Mater. Res. Bullet.* 48: 935-942.
9. Hayashi H., Hakuta Y., (2010), Hydrothermal synthesis of metal Oxide nanoparticles in supercritical water. *Materials* 3: 3794-3817.
10. Byrappa K., Adschiri T., (2007), Hydrothermal technology for nanotechnology. *Progr. Crystal Growth and Charac. Mater.* 53: 117-166.
11. Wilson J. A., Uebler J. W., LaDuca R. L., (2013), Cadmium adipate coordination polymers prepared with isomeric pyridylamide precursors: pH-dependent in situ reaction chemistry and divergent dimensionalities. *Crystal Engin. Communic.* 15: 5218-5225.
12. Wang X. L, Q, Y, Li G. C., Luan J., Lin H. Y., (2013), Effect of organic polycarboxylates on the architectures of cadmium(II) coordination polymers based on dipyrazino 2, 3-f: 22 32 -h.quinoxaline: Syntheses, crystal structures, and photoluminescence properties. *Inorg. Chimica Acta.* 399: 105-111.
13. Sun D., Han L. L., Yuan S., Deng Y. K., Xu M. Z., Sun D. F., (2013), Four new Cd(II) coordination polymers with mixed multidentate N-Donors and biphenyl-based polycarboxylate ligands: Syntheses, structures, and photoluminescent properties. *Cryst. Growth & Design.* 13: 377-385.
14. Tadjarodi A., Imani M., Kerdari H., (2013), Adsorption kinetics, thermodynamic studies and high performance of CdO cauliflower-like nanostructure on the removal of Congo red from aqueous solution. *J. Nanostruc. Chem.* 3: 51-59.
15. Tadjarodi A., Imani M., Izadi M., Shokrayian J., (2015), Solvent free synthesis of ZnO nanostructures and evaluation of their capability for water treatment. *Mater. Res. Bullet.* 70: 468-477.
16. Afkhami A., Moosavi R., (2010), Adsorptive removal of Congo red, a carcinogenic textile dye, from aqueous solutions by maghemite nanoparticles. *J. Hazard. Mater.* 174: 398-403.
17. Nakamoto K., (2009), Infrared Raman Spectra of Inorganic and Coordination Compounds, John Wiley & Sons Press. Inc. Hoboken, New Jersey.
18. Zenasni M. A., Meroufe B., Merlin A., George B., (2014), Adsorption of congo red from aqueous solution using CTAB-Kaolin from bechar algeria. *J. Surf. Engin. Mater. Adv. Tech.* 4: 332-341.
19. Nagda G. K., Ghole V. S., (2009), Biosorption of congo red by hydrogen peroxide treated tendu waste. *Iranian J. Environ. Health Sci. Eng.* 6: 195-200.
20. Wang B., Wu H., Yu L., Xu R., Lim T. T., Lou X. W., (2012), Template-free formation of uniform urchin-like á-FeOOH hollow spheres with superior capability for Water treatment. *Adv. Mater.* 24: 1111-1116.